CLINICAL SCIENCES

Epithelial-Stromal Interactions in Human Keratotomy Wound Healing

Gerrit R. J. Melles, MD; Perry S. Binder, MD; Max N. Moore; Janet A. Anderson, PhD

Objective: To evaluate epithelial-stromal interactions in the healing of stromal wounds and the relationship of such interactions to regional variations in healing throughout keratotomy wounds.

Methods: Ten radial keratotomy autopsy specimens were studied by using light and transmission electron microscopy.

Results: Underneath epithelial plugs, the epithelial-stromal interface was characterized by three adjacent morphological zones: a duplicated basement membrane complex, a zone that resembled Bowman's layer, and a third zone with collagenous fiber orientation parallel to the plugs. Scar tissue orientation was transverse at the base of the plug, and sagittal in deeper wound regions.

Conclusions: Basement membrane duplication and a Bowman's layer–like region underneath a plug may result from complicated epithelial-stromal interaction. Asymmetrical organization of the scar, with subepithelial transverse and sagittal deeper scar tissue orientation, may characterize radial keratotomy wound healing, and may relate to variations in final refractive effect.

(Arch Ophthalmol. 1995;113:1124-1130)

INCOMPLETE HEALING of corneal wounds several years after radial keratotomy may be related to residual refractive errors and traumatic wound rupture.[1,2] In the histological evaluation of human keratotomy wounds, two healing stages—possibly sequential-healing phases—have been documented.[1,3-5] A first stage is characterized by the presence of an epithelial plug in the wound, and a second stage is characterized by complete stromal wound closure with scar tissue orientation parallel to the wound. This organization of the scar may be ineffective for the recovery of tensile strength across the wound. Scar tissue organization parallel to the wound has been hypothesized to persist from initial fibroblast orientation and associated collagenous fiber deposition parallel to the epithelial plug.[1,6,7] (Myo)fibroblasts have been suggested to orient parallel to the wound in response to stress forces that may have a predominant direction along the wound edges.[8]

In two recent studies,[9,10] long-term keratotomy wounds in humans and monkeys showed a regional variation in healing. Collagenous fibers across anterior regions were found to be continuous with those in lamellae at the wound edges, resulting in a pseudolamellar, anterior wound repair. Middle and posterior regions displayed a scar tissue orientation parallel to the wound. However, because of the partial pseudolamellar repair, the organization of the scar does not seem to be explained by the current concept that scar tissue organization parallel to the wound results from early cell orientation parallel to the epithelial plug.

To evaluate how the epithelial plug is involved in the formation of the stromal scar, and to determine factor(s) that contribute to a regional variation in healing, we studied the histologic interaction between the epithelium and stroma in human keratotomy autopsy specimens.

RESULTS

Of the 20 human keratotomy wounds evaluated, all but one contained an epithelial plug, with a mean±SD stromal depth of 12.5%±6.5% (**Figure 1** and Table 1). The interface between the plug and the stromal tissue around the entire plug most often had a continuous basement membrane complex with hemidesmosomes and anchoring fibrils (**Figure 2**). Remnants of a previously deposited basement membrane complex were often seen in the adjacent scar tissue; in be-

From the Departments of Ophthalmology and Pathology, University of Nijmegen (the Netherlands) (Dr Melles), and the Ophthalmology Research Laboratory, National Vision Research Institute, San Diego, Calif (Drs Binder and Anderson and Mr Moore).

See Materials and Methods on next page

MATERIALS AND METHODS

Ten individual human radial keratotomy autopsy specimens (**Table 1**) were received through the San Diego (Calif) Eye Bank. Corneal quadrants intended for light and transmission electron microscopy were fixed in 2.5% glutaraldehyde or 2% paraformaldehyde in 0.1-μmol/L cacodylate buffer (pH 7.3, 340 mOsm), postfixed in 2% osmium tetroxide in 0.1-μmol/L cacodylate buffer for 1 hour, dehydrated in a graded series of ethanol and intermediate changes of propylene oxide, and embedded in epoxy resin (Poly bed Epon 812, Polysciences, Warrington, Pa).

All incisions were divided into central, middle, and peripheral portions (for clarity of nomenclature throughout the text, incision depth was subdivided into anterior, middle, and posterior "regions," and incision length was subdivided into central, middle, and peripheral "portions"); 1-μm sections were cut transversely to each of the incision portions. Middle portions of three wounds were sectioned parallel to the corneal surface (en face), from the epithelial to the endothelial surface. Sections were stained with Mallory's azure II–methylene blue, counterstained with basic fuchsin,[11] and photographed at 150× magnification (Vanox light microscope, Olympus Optical Co Ltd, Tokyo, Japan). Ultrathin sections were stained with 2% aqueous uranyl acetate, followed by Reynold's lead citrate. Ultrathin sections of at least one representative wound of each specimen were placed on slot grids (0.7% Formvar in ethylene dichloride, Ernest R. Fullam, Lathan, NY),[9] to allow visualization of the entire wound area with a transmission electron microscope at 75 kV (HU 11E, Hitachi, Tokyo).

In 20 keratotomy wounds (Table 1), the wound-healing morphological characteristics were evaluated by using the following parameters: (1) epithelium—presence and dimensions of an epithelial plug; (2) epithelial basement membrane—morphological features, duplication, presence of hemidesmosomes, and diameter of anchoring fibrils and microfibrils; (3) Bowman's layer—collagenous fiber diameter; and (4) scar—fibroblast orientation, presence of myofibroblastic characteristics (bundles of microfilaments, a cortical microfilament network, filaments radiating from the cell membrane, and presence of extensive rough endoplasmic reticulum, microtubules, and the Golgi complex),[12] presence of cell-cell contacts between epithelial plug cells and fibroblasts, collagenous fiber diameter, degree of collagenous fiber continuity across the wound, and presence of remnant basement membrane, Bowman's layer, and/or microfibrils in deeper scar regions.

To measure incision depth, epithelial plug depth, and thickness of transversely oriented scar tissue underneath the inferior border of the plug, as a percentage of corneal thickness, one line was drawn at the anterior surface of Bowman's layer, and a second line was drawn at the posterior edge of Descemet's membrane in photomicrographs at 250× magnification.[10] Data from the central, middle, and peripheral incision portions were averaged.

Ultrastructural measurements were performed in three adjacent zones that bordered the epithelial plug and in adjacent control tissue (**Table 2** through **Table 4**). Zone 1 was defined as a subepithelial plug layer that contained components of the basement membrane and anchoring fibril complex; zone 2 was defined as a layer underneath zone 1 that contained a random fiber organization that resembled Bowman's layer; and zone 3 was defined as a layer underneath zone 2, with fiber bundle orientation parallel to the plug (ie, sagittal at the lateral plug borders and transverse or pseudolamellar at the base of the plug).

Measurements of fiber diameter (ie, the shortest diameter of cross-sectional fiber contours on ultrastructural micrographs at a final magnification of 113 000×) were performed with a 7× reticle (Bausch & Lomb, Rochester, NY), with a 20-mm metric scale at 0.1-mm intervals; these measurements were averaged for each wound (Tables 2 through 4).[9,13] The thickness of zones 1 and 2 was measured in five representative areas at a magnification of 20 000×, by using the 4×4-cm crosshairs of the eyepiece of the transmission electron microscope, with a 8-cm metric scale at 1-cm intervals (Tables 2 and 3). Ten fiber diameter measurements were taken of microfibrils and anchoring fibrils underneath the epithelial plug and the surface epithelium (Table 2). Thirty measurements of fiber diameter were taken in zone 2 and in the anatomical Bowman's layer (Table 3). Thirty fiber diameter measurements were taken in zone 3 and in adjacent control stroma at the same stromal depth (Table 4).

Cell interaction was defined by direct cell-cell apposition of cell membranes. Fibroblasts were distinguished from epithelial cells by the lack of a basement membrane complex along the entire cell surface that faced the scar, their different cell shape and organelles, and their predominantly intrastromal orientation.[3] Cellular interactions between fibroblasts and epithelial plug cells, basement membrane duplication, fibroplasia from the wound edges that extended underneath the surface epithelium, and basement membrane remnants and microfibers in deeper scar regions were graded as absent (minus) or present (plus) (**Table 5**).

Statistical analysis was performed by using the paired Student's *t* test.

tween focal duplications of the complex, microfibrils and anchoring fibers were visible (Figure 2). Accumulation of both types of fibrils was also seen in typical recesses (anterior impressions in the "basal" epithelial plug cells) (Figure 2). Clusters of microfibrils (typically 10 to 50) were visible throughout the scar tissue in the vicinity of the plug (Figure 2), but such clusters were also found in deeper scar regions (Figure 2 and Table 5). The basement membrane complex was absent in areas where fibroblasts and epithelial cells showed direct cell-cell contacts (Figure 2 and Table 5).

The presence of basement membrane duplication, microfibrils, and epithelial anchoring fibrils directly underneath the epithelial plug cells formed a "layer" of extracellular matrix (ECM) (zone 1, Figure 2) with a mean±SD thickness of 0.2±0.1 μm (Table 2). The mean±SD diameter of anchoring fibrils underneath the plug cells (3.8±0.6 nm) differed significantly from that of adjacent microfibrils (12.4±0.6 nm) ($P<.001$), but not from that of anchoring fibrils underneath the surface epithelium between keratotomy incisions (3.7±0.6 nm) ($P>.1$) (Table 2).

Directly underneath zone 1, scar tissue with a random fiber organization resembled the normal ultrastructure of Bowman's layer, except for the presence of cells and microfibrils. This layer (zone 2, Figure 2 and **Figure 3**) intermingled with more regularly organized fiber structures (ie, preexisting tissue at the wound edges and/or newly depos-

Table 1. Light Microscopical Features in Human Keratotomy Wounds*

Specimen	Patient Age, y/ Sex†	Surgical Procedure‡	Postoperative Time, mo	Cause of Death	Average, % of Corneal Thickness: Epithelial Plug Depth	Thickness Zone 3§	Incision Depth
1‖	44/F	8 RK, R eye	3.5	...	26.3	2.0	81
					16.0	4.0	86
2	27/M	8 RK, both eyes	12	Trauma	17.5	9.5	75
					10.7	7.5	77
3	41/M	8 RK+T, both eyes	19	Trauma	14.0	3.0	75
					20.7	5.7	79
4	31/M	12 RK, both eyes	27	Trauma	0	1.3	83
					4.3	0	73
5	26/F	12 RK, both eyes	52	Drugs (Graves' disease)	17.3	NM	82
					25.3	7.6	94
6	25/M	8 RK, both eyes	...	Suicide	14.3	8.3	70
					16.7	15.3	60
7	33/F	8 RK, both eyes	...	...	4.0	13.7	82
					11.3	4.0	76
8	35/F	8 RK, both eyes	...	Drugs	20.0	9.5	65
					9.0	10.3	70
9	36/M	8 RK, both eyes	...	Suicide	8.3	12.0	77
					15.7	10.0	73
10	55/F	... RK, L eye	...	Breast cancer	3.5	3.0	66
					6.0	0	84

*RK indicates radial keratotomy procedure; T, transverse incisions; and NM, not measurable. The mean±$SD_{(n-1)}$ was 12.5%±6.5% for the epithelial plug depth, 6.7%±4.6% for the thickness zone, and 76.4%±7.8% for the incision depth.

†Specimens were taken from these patients.

‡Numbers refer to the number of incisions (eg, eight-incision RK).

§Zone 3 indicates transversely oriented scar tissue directly underneath the epithelial plug.

‖Two incisions in each specimen were evaluated.

Table 2. Ultrastructural Characteristics of Zone 1*

Specimen	Zone 1: Thickness, μm	Zone 1: Diameter of Microfibrils, nm	Zone 1: Diameter of Anchoring Fibrils, nm	Control Tissue Samples (Diameter of Anchoring Fibrils, nm)
1	0.1±0	11.4±1.5	4.6±1.2	3.7±0.6
2	0.1±0.1	11.8±1.6	3.7±0.7	3.9±0.8
3	0.2±0	12.4±2.2	5.0±0.8	4.3±0.9
4	0.1±0.1	12.1±1.7	3.9±1.0	4.8±0.9
5	0.2±0	13.0±1.4	4.0±0.9	2.9±0.4
6	0.2±0.1	12.0±3.3	3.3±0.7	3.5±0.7
7	0.2±0	12.7±2.7	3.6±0.8	3.6±0.7
8	0.2±0.1	13.4±1.8	2.9±0.6	2.7±0.7
9	0.1±0	12.7±1.8	3.6±0.8	3.8±0.8
10	0.3±0.1	NM	NM	3.5±0.6

*NM indicates not measurable. Data are given as the mean±$SD_{(n-1)}$. The number of measurements was as follows: thickness, five (zone 1); diameter of microfibrils, 10 (zone 1); and diameter of anchoring fibrils, 10 (zone 1 and control tissue samples). For all 10 specimens, the mean±$SD_{(n-1)}$ was 0.2±0.1 μm (thickness [zone 1]), 12±0.6 nm (diameter of microfibrils [zone 1]), and 3.8±0.6 and 3.7±0.6 nm (diameter of anchoring fibrils [zone 1 and control tissue samples, respectively]). Significance was $P<.001$ for the diameters of the microfibrils and anchoring fibrils (zone 1); it was $P>.1$ for the diameters of anchoring fibrils between zone 1 and the control tissue samples.

Table 3. Ultrastructural Characteristics of Zone 2*

Specimen	Zone 2: Thickness, μm	Zone 2: Diameter of Collagenous Fibers, nm	Control Tissue Samples (Diameter of Collagenous Fibers in Bowman's Layer, nm)
1	1.2±0.6	20.7±2.3	21.3±2.6
2	0.7±0.3	23.0±4.7	21.1±3.9
3	1.2±0.5	26.7±6.3	22.9±3.1
4	0.7±0.6	19.1±4.3	23.0±4.3
5	0.6±0.3	22.9±7.5	25.2±3.1
6	1.1±0.8	23.9±6.0	22.5±3.5
7	0.9±0.3	22.4±3.2	22.2±3.4
8	1.0±0.4	22.7±4.7	23.7±4.3
9	0.5±0.2	21.3±4.3	22.0±4.6
10	2.9±0.4	NM	22.9±4.1

*NM indicates not measurable. Data are given as the mean±$SD_{(n-1)}$. The number of measurements was as follows: thickness, five (zone 2); diameter of collagenous fibers, 30 (zone 2); and control tissue samples, 30. For all 10 specimens, the mean±$SD_{(n-1)}$ was 1.1±0.7 μm (thickness [zone 2]), 22.5±2.1 nm (diameter of collagenous fibers [zone 2]), and 22.6±1.2 nm (control tissue samples). Significance was at $P<.1$.

ited collagenous fiber bundles). Zone 2 had a mean±SD thickness of 1.1±0.7 μm (Table 3). The mean±SD fiber diameter in zone 2 (22.5±2.1 nm) did not differ from that of the anatomical Bowman's layer within the same specimens (22.6±1.2 nm) ($P>.1$) (Table 3).

Adjacent to zone 2, the scar tissue was oriented in three directions: along the depth of the wound (sagittal), along the length of the wound (longitudinal), and across the wound (transverse) (**Figure 4**). At the lateral borders of the plug, fibroblasts and collagenous fibers had an orientation in the sagittal-longitudinal plane (Figure 4). At the base of the plug, cells and fibers showed an orientation in the transversal-longitudinal plane (Figures 1 and 3). Transverse fibers across

the wound were found to be continuous with isodirected, ie, colinear fibers of one or more lamellae at both of the wound edges (Figure 3). The thickness of the newly formed fiber bundles varied from approximately 50% to 100% of that of normal lamellae. In en face sections, parallel to the corneal surface, these bundles were often found to be organized obliquely instead of transversely (ie, at a nonperpendicular angle to the wound edge [**Figure 5**]).

Since orientation of fibroblasts appeared to be associated with that of the collagenous fibers, the thickness of the transversely oriented scar tissue (parallel to the base of the plug) was measured at the light microscopic level. The mean±SD stromal thickness of this "transversely oriented scar tissue layer" (zone 3, Figures 1 and 3) was 6.7%±4.6% of the corneal thickness (Table 1). The mean±SD collagenous fiber diameter in zone 3 (22.7±1.1 nm) did not differ significantly from that in the adjacent control stroma (22.8±1.2 nm) ($P>.1$) (Table 4); fiber diameter variability, as determined by the SD, was always higher in zone 3 (range, 3.7 to 9.4 nm) than in the adjacent control stroma (range, 1.3 to 2.7 nm) (Table 4). Scar regions underneath zone 3 (Figures 1 and 3) showed a longitudinal and sagittal collagenous fiber orientation and large accumulations of amorphous ECM; transverse fibers were generally absent.

The ultrastructure of zones 1 through 3, at the interface of the epithelial plug and the stroma, appeared to be similar underneath plugs at various stromal depths within the same or among different specimens. Postoperative time did not correlate with epithelial plug depth or thickness of pseudolamellar repair. Only in the specimen that contained incisions at 3.5 months postoperatively did the wounds show activated fibroblasts. The other specimens had varying degrees of hypocellularity of the scars, with a quiescent appearance of the fibroblasts underneath the epithelial plug.

Underneath the surface epithelium, duplication of the epithelial basement membrane was seen in six specimens (60%) (**Figure 6** and Table 5). Fibroplasia (ie, stromal tissue proliferation through the gap in Bowman's layer) was not seen in any of the specimens (Table 5).

Table 4. Ultrastructural Characteristics of Zone 3*

Specimen	Mean±$SD_{(n-1)}$ Diameter of Collagenous Fibers, nm: Zone 3	Mean±$SD_{(n-1)}$ Diameter of Collagenous Fibers, nm: Control Tissue Samples
1	21.1±4.7	21.7±1.4
2	23.8±3.7	20.4±1.3
3	22.5±9.4	23.2±1.3
4	22.9±6.5	24.6±2.0
5	23.7±5.2	23.3±2.4
6	22.0±5.6	22.9±1.9
7	22.8±5.7	22.4±2.7
8	21.6±4.8	23.4±2.3
9	24.3±4.3	23.6±2.2
10	NM	24.6±2.4

**NM indicates not measurable. For both zone 3 and the control tissue samples, the number of measurements was 30 each. For all 10 specimens, the mean± $SD_{(n-1)}$ fiber diameters were 22.7±1.1 nm (zone 3) and 22.8±1.2 nm (control tissue samples). Significance was at $P<.1$.*

COMMENT

The process of epithelial plug elimination in unsutured wounds has been studied in rabbits.[6,13-18] Because of the lack of Bowman's layer, the tendency of the incised stroma to stretch, and an approximation toward anatomical wound restoration, long-term healing in these animals may not be representative of that in humans.[13,16,19,20] Healing in monkeys may better compare with that in humans. In two recent studies,[9,10] morphological features of unsutured wounds in humans and monkeys were found to vary over the entire wound depth. Anterior regions showed a pseudolamellar restoration, whereas the middle to posterior regions were found to be disorganized. It was hypothesized that regional variations in healing may result from differences in healing rates throughout the wound, from mechanical or biochemical factors associated with epithelial plug elimination, or from different intrinsic healing properties among stromal layers.[9] In the present study, the stromal-healing response to an epithelial plug was compared between the anterior (wounds with superficial plugs) and the middle and posterior stroma (wounds with deep plugs), to analyze the epithelial-stromal interface and to determine how an asymmetrical organization of the scar in unsutured wounds is established.

Table 5. Ultrastructural Characteristics of Human Keratotomy Wounds*

Specimen	Surface Epithelium: Fibroplasia	Surface Epithelium: Duplication of Basement Membrane	Scar: Basement Membrane Remnants	Scar: Presence of Clusters of Microfibrils	Scar: Cell-Cell Contact†
1	−	−	+	+	+
2	−	−	−	+	+
3	−	+	+	+	+
4	−	−	+	+	+
5	−	+	+	+	+
6	−	+	+	+	+
7	−	−	+	+	+
8	−	+	−	+	+
9	−	+	−	+	+
10	−	+	+	+	+

**Minus sign indicates absent; plus sign, present.*
†Direct cell-cell contact between fibroblast and epithelial plug cells.

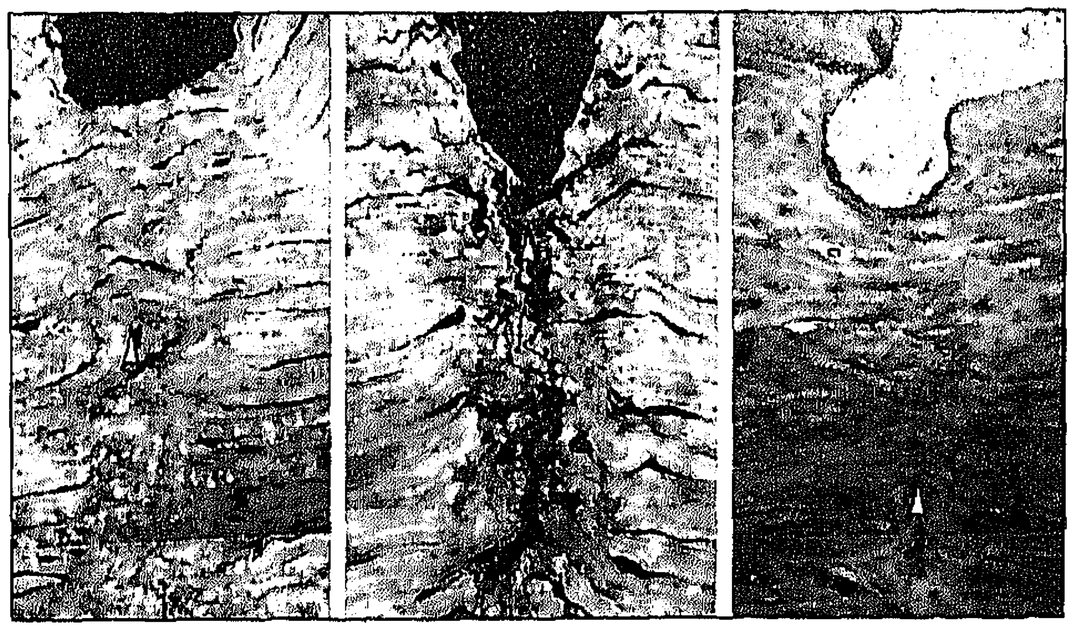

Figure 1. *Human keratotomy wounds containing epithelial plugs at 46% (left), 18% (center), and 7% (right) stromal depths (specimens 5, 1, and 7, respectively). The area with the transverse scar tissue organization directly underneath the base of the plug is indicated by an arrowhead; deeper wound regions show disorganization of cells and extracellular matrix (Mallory's azure II–methylene blue with basic fuchsin counterstain, ×750).*

All human keratotomy specimens showed three subepithelial zones by which the scar tissue that immediately surrounded the plug was characterized, irrespective of the stromal depth of the plug. A first zone that contained duplication of the basement membrane (Figure 2) has been suggested to result from the retention of the epithelium within the wound,[5,16,21] since duplication of the basement membrane was found in a variety of pathological conditions and with increasing age.[22,23] It is unknown how the continuous, centripetal epithelial movement[24] is affected by the presence of an incision(s); that is, do limbal epithelial cells enter the peripheral end of a radial incision to move the bottom of that incision toward the center, or does the epithelial sheet move over the incision at the level of Bowman's layer? A disruption of the epithelial movement with incomplete replacement of the cells within the wound could also relate to an altered basement membrane deposition.

Microfibrils that were adjacent to the epithelial plug in abundant clusters (Figure 2) may morphologically resemble preelastic, oxytalan fibrils.[25,26] In the developing cornea, microfibrils are located in the stroma, suggesting the production of these fibrils by fibroblasts.[27] The fibrils are relatively sparse in the adult, but are common in pathological conditions that involve scar tissue formation underneath the surface epithelium (eg, keratoconus and Fuchs' endothelial dystrophy).[26,28] In our study, the presence of microfibrils and anchoring fibrils over focal, duplicated (or remnant) basement membrane[29] may suggest ECM deposition over the basement membrane and subsequent formation of a new basement membrane over this ECM by epithelial cells.[26] Extracellular matrix deposition by fibroblasts would be expected to occur underneath instead of onto the basement membrane; in areas with direct contact between epithelial and stromal cells, the basement membrane was always absent (Figure 2). An epithelial cell response to surgical wounding was also suggested by basement membrane duplication underneath the surface epithelium in areas between wounds (Figure 6).[5,21] However, this duplication may have been preexistent or induced by surgical manipulation of the wound edges.[1,30]

Underneath the first zone, a second zone contained a random fiber structure that resembled the anatomical Bowman's layer (Figures 2 and 3). The presence of cells and their close interaction with microfibrils suggested that this

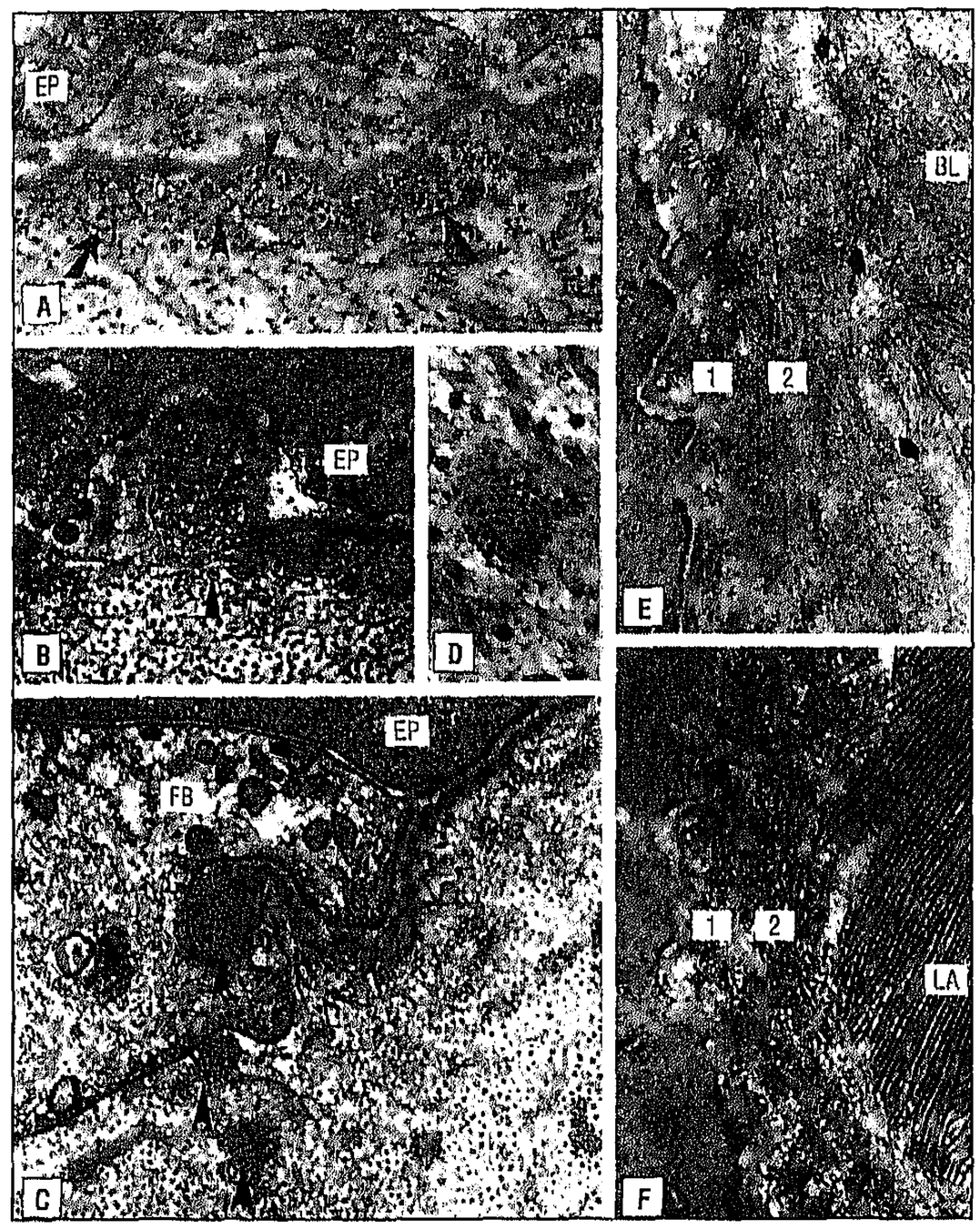

Figure 2. *Transmission electron microscopy of the characteristic features of zones 1 and 2 (specimens 3 [A], 7 [B], 2 [C], 2 [D], 6 [E], and 5 [F]). A, The epithelial plug (EP) is bordered by a basement membrane complex with hemidesmosomes (asterisks), anchoring fibers (small arrowheads), and microfibrils (large arrowhead). The complex shows duplication and can be distinguished from the adjacent scar tissue (zone 1, arrows). B, Within a typical epithelial "recess," accumulation of hemidesmosomes (asterisk), anchoring fibers (small arrowheads) and microfibrils (large arrowhead) can be seen. C, Direct cell-cell contact (small arrows) is visible between a fibroblast (FB) and an EP cell. Note that a basement membrane complex is present underneath the EP cell, but not underneath the FB cell membrane facing the scar. Underneath the basement membrane and throughout the adjacent scar tissue, clusters of microfibrils (arrowheads) are visible. D, A cluster of microfibrils is seen in deeper scar regions underneath the EP. E and F, Adjacent to the lateral border of the EP, in between zone 1 (1) and the anatomical Bowman's layer (BL, small arrows) and a stromal lamella (LA), a scar tissue layer (zone 2 [2]) can be seen with a BL-like random fiber organization (uranyl acetate–lead citrate, ×39 000 [A], ×43 000 [B], ×52 500 [C], ×101 000 [D], and ×34 000 [E, F]).*

zone of fibrous tissue had replaced epithelial cells of the plug or their basement membrane meshwork, and that it formed a transition zone between the epithelium and the underlying scar tissue that was organized parallel to the plug.

A transverse scar tissue orientation at the base of the plug in the present study (Figures 1 and 3) may resemble the previously described[9] subepithelial pseudolamellar repair in the anterior regions of completely healed keratotomy wounds. Furthermore, in a recent monkey study,[31] the former presence of an epithelial plug in unsutured wounds apparently resulted in an initial transverse scar tissue orientation over the entire wound depth, whereas the scar was disorganized in early sutured wounds. These observations suggest that transverse scar tissue organization is induced by (factors related to) the epithelial plug. To what extent can the epithelium direct fibroblast and associated collagen fiber orientation?

Fetal chick epithelium (ectoderm) may produce an acellular "primary stroma" that serves as a directional membrane for neuroectodermal fibroblast invasion.[32] In subsequent

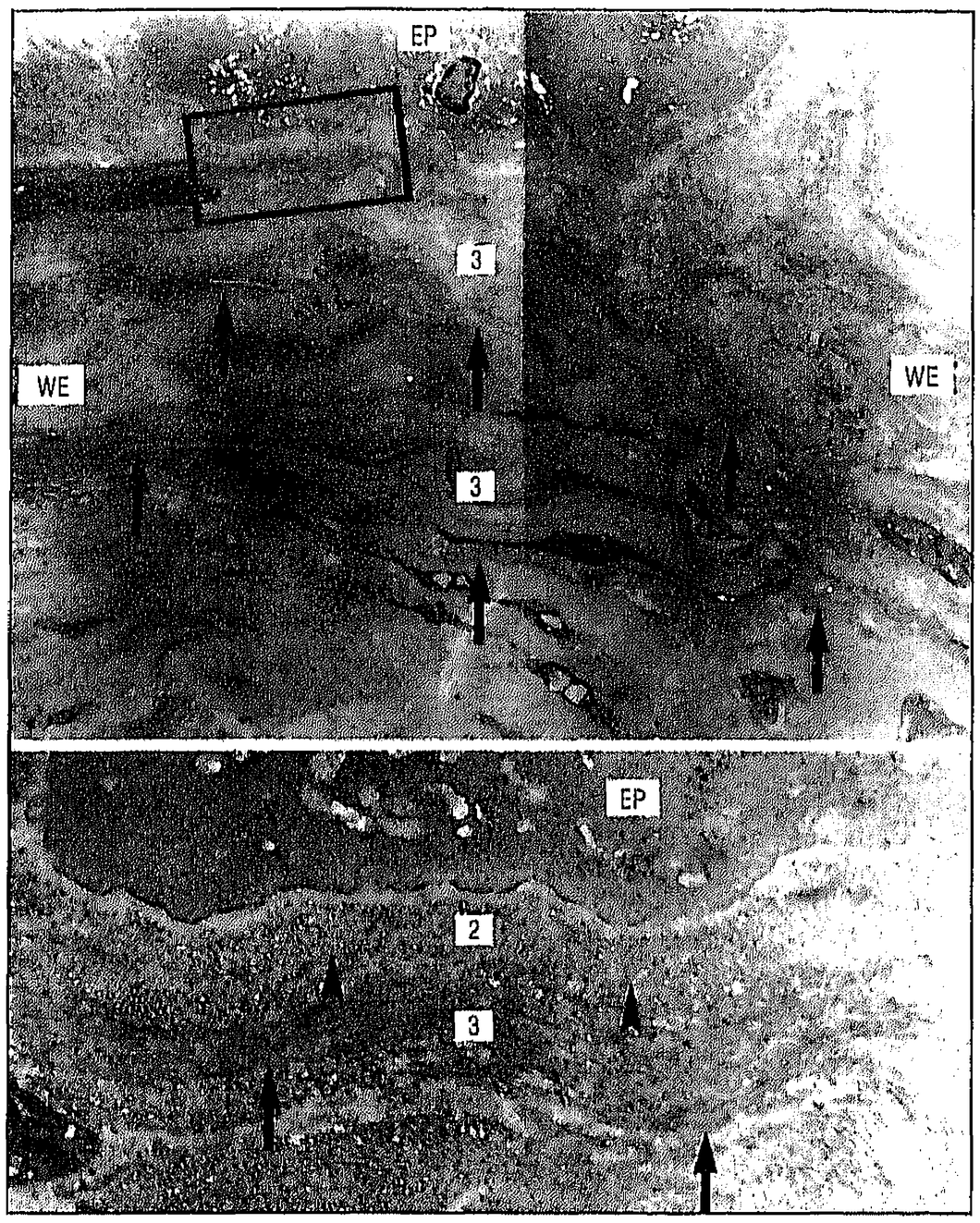

Figure 3. *Transmission electron microscopy of characteristic scar tissue organization in zone 3 (3) of a human keratotomy wound (specimen 5). Top, Underneath the base of the epithelial plug (EP) at 43% stromal depth, transverse fibroblast orientation is visible. Bundled collagenous fibers across the wound (arrows) appear to be continuous with isodirected fibers of one or more lamellae at the wound edges (WE) (uranyl acetate–lead citrate, ×3000). Bottom, Higher magnification of the area indicated at top. Directly underneath the EP, a layer of scar tissue resembling the anatomical Bowman's layer can be seen (zone 2 [2], arrowheads). Adjacent to zone 2, transversely oriented fibers (arrows) are visible that characterize zone 3 (3) (uranyl acetate–lead citrate, ×15 000).*

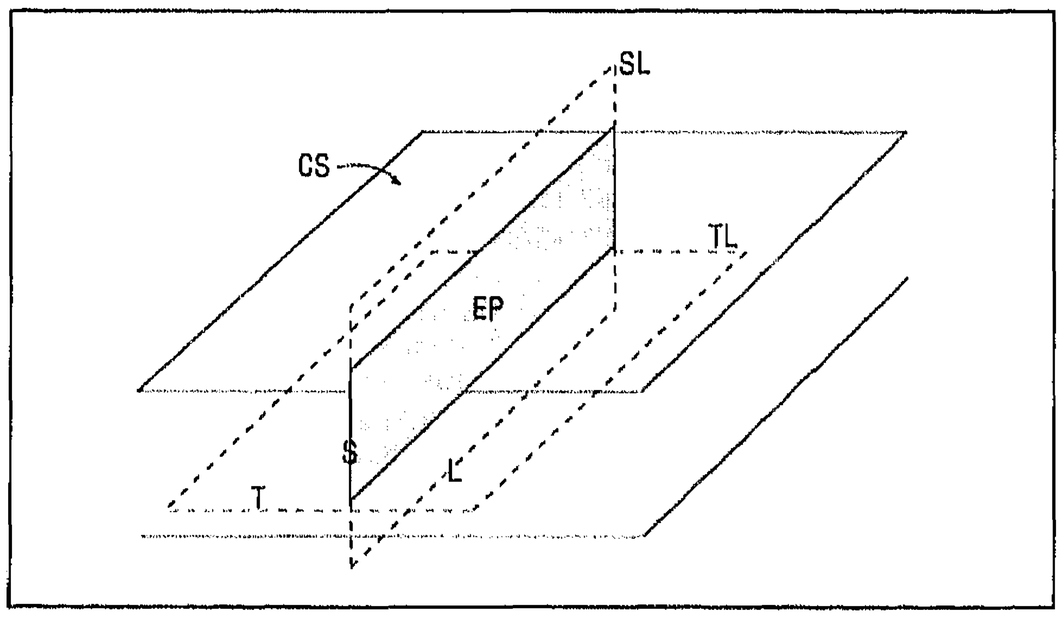

Figure 4. *Diagram that explains terminology of scar tissue orientation. Fibroblast and collagenous fiber orientation is defined as sagittal (S [along wound depth]), longitudinal (L [along wound length]), or transverse (T [across the wound]). Of the three zones at the interface between the epithelial plug (EP) and stroma, the third zone had fibroblast and collagenous fiber orientation parallel to the EP: at the lateral borders of the plug, scar tissue was organized in the "SL" plane, and at the inferior border, it was organized in the "TL" plane. The shaded area represents the orientation of the EP within the wound perpendicular to the corneal surface (CS).*

phases of development, these fibroblasts may deposit collagen onto the primary fibers to form a "secondary stroma."[33] In vertebrates, the primary stroma may have a limited capacity to serve as a directional membrane for lamellar fibroblast organization.[32,34] Although a recapitulation of fetal tis-

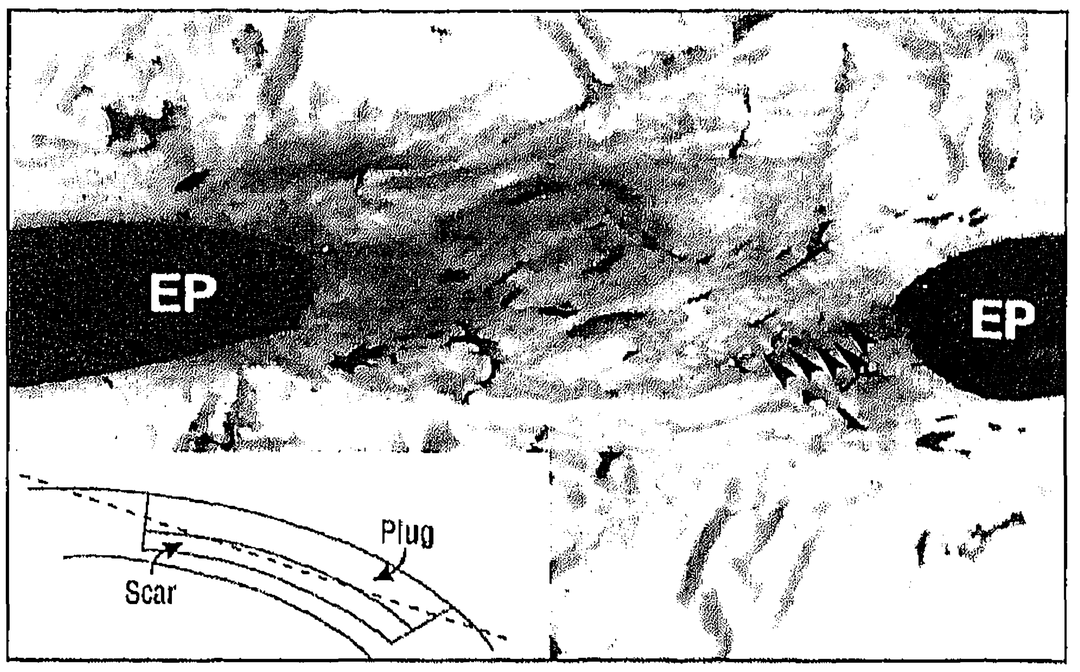

Figure 5. *"En face" section made parallel to the corneal surface of a human keratotomy wound (specimen 8). Directly underneath the epithelial plug (EP), fiber bundles (arrowheads) can be discerned in an oblique direction across the wound. Although the direction of collagenous fiber bundles was determined at an ultrastructural level, the orientation of the fiber bundles to the wound axis is better shown at a light microscopical level. Inset, Dotted line represents the plane of sectioning (Mallory's azure II–methylene blue with basic fuchsin counterstain, ×310).*

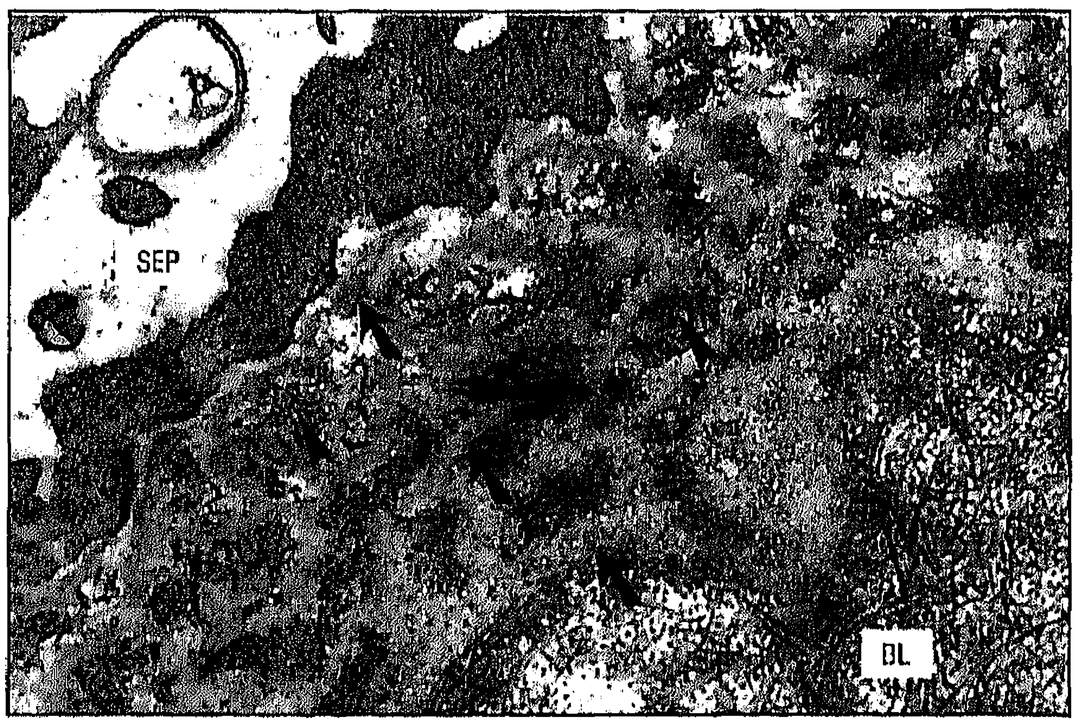

Figure 6. *Transmission electron microscopy of a human keratotomy wound (specimen 5). Underneath the surface epithelium (SEP), multiple duplications of the basement membrane (arrows) and accumulations of anchoring fibers (arrowheads) are visible. BL indicates Bowman's layer (uranyl acetate–lead citrate, ×41 000).*

sue conditions has been documented[13,35] in healing wounds, the role of epithelial ECM deposition in fibroblast direction may be uncertain. However, the borders of the epithelial plug may be expected to serve as a "new corneal surface" for template-depending fibroblasts.[1,7,36,37] If so, the capacity of the plug to induce fibroblast orientation parallel to its inferior border may result in a pseudolamellar scar tissue organization across the wound. Apparently, induction of transversely oriented scar tissue by the plug is limited to the area directly underneath the plug, since deeper regions contained a sagittal scar tissue organization.

Alternatively, (myo)fibroblasts may orient according to stress lines within the tissue.[8,12,16] In keratotomy wounds in cats, myofibroblasts had an orientation parallel to the corneal surface, but not necessarily across the wound.[38] In keratotomy wounds in rabbits, myofibroblasts showed a reorientation from a random distribution into an orientation along the wound.[8] It was hypothesized that the stress forces along the wound exceeded those across the wound, so that the cells reoriented along the wound. In the present study, the orientation of subepithelial fibroblasts and codirected collagenous fibers parallel to the corneal surface but at variable

angles to the wound edge (Figure 5) may therefore suggest that the major stress forces were directed in the transversal-longitudinal corneal plane (Figure 4). If so, the stress forces apparently concentrate in the area directly underneath the epithelial plug, because the scar tissue in deeper wound regions had a sagittal orientation and seemed therefore not to be subjected to or organized by stress forces across the wound.

Apart from its causative factors, the presence of a thin layer of subepithelial pseudolamellar repair at a given stromal depth may be expected to have an effect on the stress-bearing qualities of an individual wound.[39,40] These properties may be hypothesized to vary with the depth of the epithelial plug and the thickness of the layer of pseudolamellar repair: the more anterior the pseudolamellar repair, the more wound stability; and the thicker the pseudolamellar repair, the more wound strength. Extreme individual wound-healing responses,[4,5] eg, a thick pseudolamellar layer underneath a superficial epithelial plug, may clinically result in less refractive effect (ie, undercorrection), and a thin layer underneath a deep plug may result in more effect and refractive instability (ie, overcorrection or fluctuation in visual acuity). Because incision depth, the depth of the plug, and the thickness of the pseudolamellar repair varied among the incisions within the same specimens, each of the incisions may have had a different contribution to the refractive effect.

The presence of transversely oriented scar tissue directly underneath the epithelial plug, but not in deeper scar regions, indicated that the healing of unsutured wounds is characterized by a regional variation in healing. Since pseudolamellar repair was found underneath plugs at different stromal levels, asymmetry of the scar appeared to be independent of the presence and the depth of a plug. Epithelial plug(s) at a variable stromal depth and associated pseudolamellar repair of variable thickness may affect the biomechanical response of the cornea following radial keratotomy, and the response may change during elimination of the plug(s) from the wound(s) or during scar remodeling.

Accepted for publication April 28, 1995.

This study was supported by grants from the Department of Ophthalmology, University of Nijmegen (the Netherlands), and from the National Vision Research Institute, San Diego, Calif.

M. E. Rock, National Vision Research Institute; F. J. R. Rietveld, Department of Ophthalmology, University of Nijmegen; N. SundarRaj, PhD, The Eye and Ear Institute, Pittsburgh, Pa; and J. Hermans, PhD, Department of Medical Statistics, University of Leiden (the Netherlands), provided advice and cooperation.

Correspondence to Department of Ophthalmology, University of Nijmegen, Philips van Leydenlaan 15, PB 9101, 6500 HB Nijmegen, the Netherlands (Dr Melles).

REFERENCES

1. Binder PS. What we have learned about corneal wound healing from refractive surgery. *J Refract Corneal Surg.* 1989;5:98-120.
2. Rashid ER, Waring GO. Complications of refractive keratotomy. In: Waring GO, ed. *Refractive Keratotomy for Myopia and Astigatism.* St Louis, Mo: Mosby–Year Book; 1992:863-936.
3. Binder PS, Wickham MG, Zavala EY, Akers PA. Corneal anatomy and wound healing. In: *Transactions of the New Orleans Academy of Ophthalmology.* St Louis, Mo: CV Mosby Co; 1980:1-35.
4. Melles GRJ, Binder PS. A comparison of wound healing in sutured and unsutured corneal wounds. *Arch Ophthalmol.* 1990;108:1460-1469.
5. Jester JV, Villaseñor RA, Schanzlin DJ, Cavanagh HD. Variations in corneal wound healing after radial keratotomy. *Cornea.* 1992;11:191-199.
6. Cintron C, Szamier RB, Hassinger LC, Kublin CL. Scanning electron microscopy of rabbit corneal scars. *Invest Ophthalmol Vis Sci.* 1982;23:50-63.
7. Coalwell KA, Binder PS. High voltage electron microscopic analysis of wound healing after human radial keratotomy. *Invest Ophthalmol Vis Sci.* 1988;29(suppl):280.
8. Petroll WM, Cavanagh HD, Barry P, Andrews P, Jester JV. Quantitative analysis of stress fiber orientation during corneal wound contraction. *J Cell Sci.* 1993;104:353-363.
9. Melles GRJ, Binder PS, Anderson JA. Variation in healing throughout the depth of long-term, unsutured, corneal wounds in human autopsy specimens and monkeys. *Arch Ophthalmol.* 1994;112:100-109.
10. Melles GRJ, Binder PS. Effect of wound location, orientation, direction and postoperative time on unsutured corneal wound healing morphology in monkeys. *J Refract Corneal Surg. 1992;8:427-438.*
11. Rock ME, Anderson JA, Binder PS. A modified trichrome stain for light microscopic examination of plastic embedded corneal tissue. *Cornea.* 1993;12:255-260.
12. Jester JV, Rodrigues MM, Herman IM. Characterization of avascular corneal wound healing fibroblasts. *Am J Pathol.* 1987;127:140-148.
13. Cintron C, Hassinger LC, Kublin CL, Cannon DJ. Biochemical and ultrastructural changes in collagen during corneal wound healing. *J Ultrastruct Res. 1978; 65:13-22.*
14. Goodman WM, SundarRaj N, Garone M, Arffa RC, Thoft RA. Unique parameters in the healing of linear partial thickness penetrating corneal incisions in rabbits: immunohistochemical evaluation. *Curr Eye Res.* 1989;8:305-316.
15. Davison PF, Galbavy EJ. Connective tissue remodeling in corneal and scleral wounds. *Invest Ophthalmol Vis Sci.* 1986;27:1478-1484.
16. Jester JV, Petroll WM, Feng W, Esseplan J, Cavanagh HD. Radial keratotomy, I: the wound healing process and measurement of incisional gape in two animal models using in vivo confocal microscopy. *Invest Ophthalmol Vis Sci.* 1992; 33:3255-3270.
17. Matsuda H, Smelser GK. Electron microscopy of corneal wound healing. *Exp Eye Res.* 1973;16:427-442.
18. Cintron C, Schneider H, Kublin C. Corneal scar formation. *Exp Eye Res.* 1973; 17:251-259.
19. Lee RE, Davison PF, Cintron C. The healing of linear nonperforating wounds in rabbit corneas of different ages. *Invest Ophthalmol Vis Sci.* 1982;23:660-665.
20. Yamaguchi T, Tamaki K, Nakata S, Nakajima A, Kaufman HE. Long-term histologic evaluation of wound healing after anterior radial keratotomy in rabbits. *Invest Ophthalmol Vis Sci.* 1988;29(suppl):391.
21. Jester JV, Villaseñor RA, Miyashiro J. Epithelial inclusion cysts following radial keratotomy. *Arch Ophthalmol.* 1983;101:611-615.
22. Kenyon KR. Morphology and pathologic responses of the cornea to disease. In: Smolin G, Thoft RA, eds. *The Cornea: Scientific Foundations and Clinical Practice.* Boston, Mass: Little Brown & Co Inc; 1987:63-98.
23. Alvarado J, Murphy C, Juster R. Age-related changes in the basement membrane of the human corneal epithelium. *Invest Ophthalmol Vis Sci.* 1983;24:1015-1028.
24. Thoft RA, Friend J. The X, Y, Z hypothesis of corneal epithelial maintenance. *Invest Ophthalmol Vis Sci.* 1983;24:1442-1443.
25. Binder PS, Nayak SK, Deg JK, Zavala EY, Sugar J. An ultrastructural and histochemical study of long-term wound healing after radial keratotomy. *Am J Ophthalmol.* 1987;103:432-440.
26. Alexander RA, Garner A. Oxytalan fibre formation in the cornea: a light and electron microscopical study. *Histopathology.* 1977;1:189-199.
27. Cintron C, Covington H, Kublin CL. Morphogenesis of rabbit corneal stroma. *Invest Ophthalmol Vis Sci.* 1983;4:543-556.
28. Carlson EC, Waring GO. Ultrastructural analyses of enzyme-treated microfibrils in rabbit corneal stroma. *Invest Ophthalmol Vis Sci.* 1988;29:578-585.
29. Gipson IK, Spurr-Michaud S, Tisdale AS, Keough M. Reassembly of the anchoring structures of the corneal epithelium during wound repair in the rabbit. *Invest Ophthalmol Vis Sci.* 1989;30:425-434.
30. Nelson JD, Williams P, Lindstrom RL, Doughman DJ. Map-fingerprint-dot changes in the corneal epithelial basement membrane following radial keratotomy. *Ophthalmology.* 1985;92:199-205.
31. Melles GRJ, SundarRaj N, Binder PS, et al. Epithelial-stromal interactions in unsutured and sutured wounds within the same monkey cornea. *Invest Ophthalmol Vis Sci.* 1993;34(suppl):2184.
32. Hay ED. Development of the vertebrate cornea. *Int Rev Cytol.* 1980;63:263-322.
33. Bard JBL, Higginson K. Fibroblast-collagen interactions in the formation of the secondary stroma of the chick cornea. *J Cell Biol.* 1977;74:816-827.
34. Ozanics V, Rayborn M, Sagun D. Observations on the morphology of the developing primate cornea. *J Morphol.* 1977;153:263-298.
35. Cintron C, Kublin CL. Regeneration of corneal tissue. *Dev Biol. 1977;61:346-357.*
36. Clark P, Connolly P, Curtis ASG, Dow JAT, Wilkinson CDW. Cell guidance by ultrafine topography in vitro. *J Cell Sci.* 1991;99:73-77.
37. Oster GF, Murray JD, Harris AK. Mechanical aspects of mesenchymal morphogenesis. *J Embryol Exp Morphol.* 1983;78:83-125.
38. Garana RMR, Petroll WM, Chen WT, et al. Radial keratotomy, II: role of the myofibroblast in corneal wound contraction. *Invest Ophthalmol Vis Sci.* 1992; 33:3271-3282.
39. Viola RS, Kempski MH, Nakada S, del Cerro M, Aquavella JV. A new model for evaluating corneal wound strength in the rabbit. *Invest Ophthalmol Vis Sci.* 1992;33:1727-1733.
40. Hjortdal JO. Influence of radial keratotomy on the regional mechanical performance of the human cornea. *Invest Ophthalmol Vis Sci.* 1994;35:1790.